Hindawi
Wireless Communications and Mobile Computing
Volume 2019, Article ID 3906483, 14 pages
https://doi.org/10.1155/2019/3906483

Research Article

A Data Forwarding Approach for Fire-Rescue Scenario with Multi-Type Mobile Nodes

Linfeng Liu,[1,2,3] **Ping Zhou**,[1,3] **Jiagao Wu**,[1,3] **Ran Wang**,[4] **Xiaojun Fan**,[1,3] **and Haiting Zhu**[1]

[1]*School of Computer Science and Technology, Nanjing University of Posts and Telecommunications, Nanjing 210023, China*
[2]*School of Computer and Information, Hohai University, Nanjing 211100, China*
[3]*Jiangsu Key Laboratory of Big Data Security and Intelligent Processing, Nanjing University of Posts and Telecommunications, Nanjing 210023, China*
[4]*College of Computer Science and Technology, Nanjing University of Aeronautics and Astronautics, Nanjing 211106, China*

Correspondence should be addressed to Linfeng Liu; liulinfeng@gmail.com

Received 24 February 2019; Revised 2 June 2019; Accepted 18 June 2019; Published 4 July 2019

Academic Editor: Mauro Femminella

The opportunistic mobile sensor network has been extensively applied in various public safety applications such as the fire rescue and earthquake rescue, since it can provide a surveillance range with an inexpensive cost and avoid the dangers of humans staying in risk zones. However, due to some environmental events such as building structure damage, airflow push, and fire explosions, the sensor nodes sprinkled into the fire-rescue scenario may be kept moving. Thus, the contacts between nodes become momentary, and the data packets cannot be forwarded along stable communication paths. To this end, the opportunistic forwarding manner is adopted in the fire-rescue scenario to enable the data packets to be transferred to the rescue control center (RCC) through some discrete hops. The contributions of this paper are threefold. First, the nodes in the fire-rescue scenario are carefully investigated and classified into four types: small-range mobile nodes (SRNs), large-range mobile nodes (LRNs), firefighter nodes (FNs), and robot nodes (RNs). Second, we formulate the data forwarding problem, and the optimal proportions of SRNs, LRNs, and FNs in data holders are mathematically analyzed to obtain the maximum delivery ratio. Third, a data forwarding approach for fire-rescue scenario (DFAFR) is proposed. In DFAFR, the optimal proportions of SRNs, LRNs, and FNs in data holders are maintained as far as possible through selecting different types of data holder candidates, and then the new data holders are determined from these data holder candidates and the adjacent RNs on basis of their expected delivery delay. Finally, the performance of DFAFR is analyzed through simulations of the fire-rescue scenario, and the results indicate that DFAFR can enhance the delivery ratio and shorten the delivery delay while the forwarding overhead is restricted.

1. Introduction

With the broad deployment of mobile sensor nodes, opportunistic mobile sensor networks (OMSNs) [1, 2] are introduced to achieve large-scale sensing at a lower cost compared with a ubiquitous static infrastructure of sensing devices. However, due to the node mobility, the contacts between nodes may be scarce and momentary, leading to unstable communication paths. Opportunistic data forwarding approach enables a data packet to be transferred from the source to the destination through several discrete hops, even when such a stable path never emerges.

The OMSN technology has been applied to various emergency-response applications, such as fire rescue [3, 4], earthquake rescue and mine accident rescue. In this paper, we focus on the fire-rescue scenario where the information containing the survival positions, area temperatures and fire explosions is capsuled into some data packets which need to be forwarded to the rescue control center (RCC) rapidly. As depicted in Figure 1, the fire behaviors are monitored by sensor nodes sprinkled by firefighters who move on for the rescue work, and this way of deploying nodes has been mentioned as a breadcrumb system in [5], where the breadcrumbs (sensor nodes) are deployed automatically on

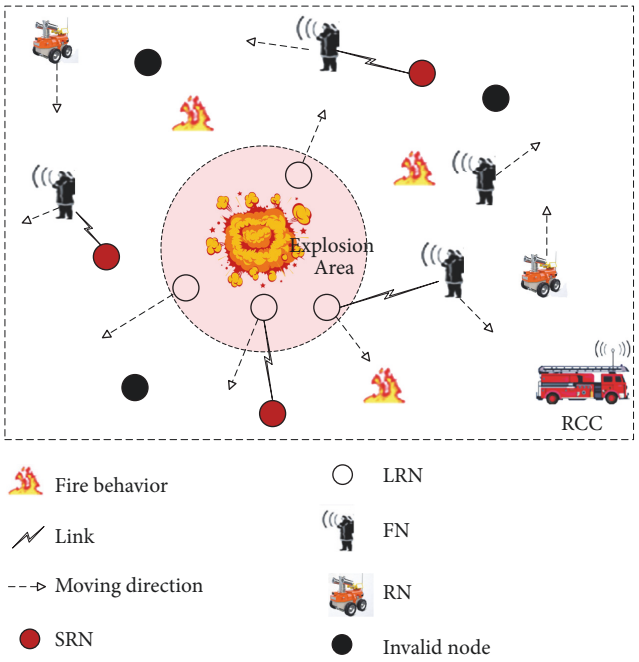

Figure 1: An OMSN for fire-rescue scenario.

the fly when the firefighters run into the burning buildings. Then, the data packets containing the information of fire behaviors are forwarded to the RCC through intermittent multi-hop communications. The OMSN in fire-rescue scenario is composed of four types of nodes: (a) the small-range mobile nodes (SRNs) are located far from fire explosions, and they move slowly; (b) the large-range mobile nodes (LRNs) can bounce away from current positions due to the nearby combustion explosions or building structure damage [6], and thus their positions can be altered abruptly; (c) the firefighter nodes (FNs) are carried by firefighters who usually perform purposive movements, so that the FNs are considered to move regularly; (d) the robot nodes (RNs) traverse the fire area according to a predefined rule, such as the rule introduced in Section 3.1. Note that an SRN (or an LRN) can be transformed into an LRN (or an SRN) due to its surrounding fire behaviors; besides, SRNs, LRNs, FNs or RNs can be transformed into invalid nodes when they are destroyed in the fire-rescue scenario.

The data forwarding technique in the fire-rescue scenario is defined as the art of mobile nodes disseminating the data packets to RCC through intermittent multi-hop links. Due to the intermittent contacts between nodes, the data delivery quality cannot be guaranteed even though the epidemic forwarding is adopted. Hence, how to enhance the delivery ratio in the fire-rescue scenario is a vital issue. Besides, a data packet delivered to RCC more rapidly is believed to provide more valuable references about the fire behaviors for further decisions, and thus how to shorten the delivery delay becomes another critical issue. To enhance the delivery ratio and shorten the delivery delay, a data forwarding approach for OMSN in the fire-rescue scenario is proposed and thoroughly evaluated in this paper. In our work, the mobility patterns of SRNs, LRNs, FNs and RNs are modeled, and the optimal proportions of SRNs, LRNs and FNs in data holders are analyzed to maximize the delivery ratio. Furthermore, the new data holders are selected from the data holder candidates and the adjacent RNs to shorten the delivery delay.

The remainder of this paper is organized as follows: Section 2 briefly surveys some existing related studies. Section 3 proposes a network model to describe the opportunistic data forwarding problem, and then the delivery delay and delivery delay are analyzed. Section 4 presents an opportunistic data forwarding approach for the fire-rescue scenario (DFAFR). Simulation results for performance evaluation of DFAFR are reported in Section 5. Finally, Section 6 concludes the paper.

This work is a significant extension of our early work [7]. Specifically, we introduce the RNs into the network model, and the new data holders will be determined from the data holder candidates and the adjacent RNs according to their expected delivery delay. The external forces in combustion process are analyzed to derive the mobility patterns of SRNs and LRNs, which are closer to the real fire-rescue scenario. Besides, more simulation results are also provided to further clarify the merits of the proposed DFAFR.

2. Related Work

Recently, the opportunistic data forwarding problem in mobile sensor networks has attracted a lot of interest. In the early representative work, Direct Transmission (DT) [8], each data packet is forwarded until the data holder encounters the destination node, and thus the data packet will not be copied, and this mechanism leads to a very low delivery ratio. It is obvious that DT is with the minimum expense, despite an unsatisfactory delivery ratio and a very long delivery delay. On the contrary, in Epidemic Forwarding (EF) [9], each node forwards the held data packets to all the encountered nodes. EF can achieve a large delivery ratio and a short delivery delay, but it usually produces massive data packet copies and causes the network congestion easily. In [10], based on the calculated forwarding probabilities, the Probabilistic Routing Protocol using History of Encounters and Transitivity (PROPHET) provides a mobility prediction of nodes to help the data dissemination. The performance of PROPHET relies on the movement regularity of nodes.

With regard to the mobility patterns, there are some typical mobility models, as the Brown model, random waypoint model, random walk model, random direction model, reference point group mobility and so on [11–13]. Besides, some mobility models have been proposed for the disaster scenarios. In [14], Joe et al. assume that an earthquake has occurred in a city where some roads and nodes have been damaged. A Message Priority Routing Protocol (MPRP) is proposed to remedy the performance degradation caused by these damage, and MPRP is able to deliver more messages to the destination in the earthquake-scenario. Reference [15] is based on the Post Disaster Mobility model (PDM), which captures the mobility features of humans or vehicles in disaster rescue scenarios. In PDM, vehicles carrying supplies may move between the coordination centers and evacuation camps. A number of rescue workers and volunteers are dedicated to locate survivors and offer help. Reference

[15] also raises an inter-contact routing method where the delivery delay and delivery ratio can be estimated. Likewise, Aschenbruck *et al*. propose a disaster area mobility model in [16], where the characteristics of public safety communication networks such as heterogeneous area-based movement, obstacles and joining/leaving of nodes are provided. In [17], a health care Small-World Network (SWN) evolves naturally from social interactions and population dynamics. However, during a crisis, the SWN is constrained by interrupted transportation within the limited geographic topology. Reference [18] proposes an opportunistic data transmission mechanism based on a susceptible-infected model, and this model is used to analyze the social characteristics of mobile crowd sensing networks and obtain the table of evolutionary relationships between nodes. The evolutionary relationships are quantified and added to the opportunistic routing as additional information, to guide the nodes to reach the destination successfully. Combining random waypoint and random direction model, [19] presents a novel earthquake relief mobility model through analyzing the demand characteristics of earthquake relief within a prime time. In [20], a learning automata-based multi-level heterogeneous routing is designed for energy conservation. [21] presents an SDN-based scheme to make intelligent decisions for data offloading, and it is verified that the traffic routing is managed efficiently even with an increase in the network size.

Tabirca et al. construct a dynamic model for the fire emergency evacuation problem, and the model redefines the concept of safety [22]. To establish emergency communication networks for fire-fighting in underground buildings, a reliable fire emergency communication network is designed to realize the QoS communications and guarantee the stability of communication performance [23]. Besides, a fire emergency and gas detection system based on WSNs for both indoor and outdoor environments is given in [24], where the modules of sensing duties, network-node interactions, and system resiliency are integrated into this system. In [25], a localization and tracking system based on the usage of IEEE 802.11 technology is provided for augmenting the GPS coverage in emergency scenarios. Likewise, [26] proposes a localization and tracking system based on the combined usage of WiFi and GPS for emergency scenarios, and this system is characterized by ease of deployment and usage, since it does not require any particular configurations.

In the fire-rescue scenario, the fire behaviors can be monitored by some sensor nodes and then encapsulated into some data packets, which are then transmitted to RCC through intermittent multi-hops. However, the typical mobility patterns of nodes in fire-rescue scenario have not been investigated and concluded in existing works, and the mobility patterns of nodes should be considered in the selection of data holders. In this paper, the typical mobility patterns in fire-rescue scenario will be concluded according to the movement features of nodes, and then a data forwarding approach is designed for the fire-rescue scenario with multi-type mobile nodes.

Table 1: Description of main notations.

Parameter	Description
R_c	Communication range of each node
ρ_s	Proportion of SRNs in data holders
ρ_l	Proportion of LRNs in data holders
ρ_f	Proportion of FNs in data holders
v_s	Movement speed of SRNs
v_f	Movement speed of FNs
v_r	Movement speed of RNs
t_s	Residence period of an SRN at each time slot
t_l	Residence period of an LRN after each bounce
t_f	Residence period of an FN at each time slot
r_e	Explosion range
r_l	Maximum bounce range
L_s	Size of each data packet
$\mathcal{T}$	Forwarding deadline of each data packet
κ	Number of forwarded copies at each time slot
$C(i)^t$	Coordinate of V_i at the t-th time slot
$d_p(i,j)^t$	Position alteration between V_i and V_j at the t-th time slot
$S_p(i)^t$	Position stability of V_i at the t-th time slot
$\mathscr{D}_s{}^t$	Delivery ratio with SRNs at the t-th time slot
$\mathscr{D}_l{}^t$	Delivery ratio with LRNs at the t-th time slot
$\mathscr{D}_f{}^t$	Delivery ratio with FNs at the t-th time slot
$\mathscr{D}^t$	Delivery ratio with SRNs, LRNs and FNs at the t-th time slot

3. Analysis Framework

Suppose that N mobile nodes are uniformly deployed in a fire area $\mathbf{A}$ ($\mathbf{A} \in \mathbb{R}^2$). The time is divided into discrete time slots with an equal length τ. Each node (except the invalid nodes) is assumed to be equipped with a GPS equipment, and thus it can obtain the real-time coordinate. The objective of data forwarding problem is to enhance the delivery ratio and shorten the delivery delay while the forwarding overhead is restricted. Note that the energy consumption is confined as well by restricting the number of forwarded copies (forwarding overhead), because the energy consumption is mainly produced by the data dissemination. The explanations of the main notations are presented in Table 1.

3.1. Mobility Patterns of Nodes. In the fire-rescue scenario, suppose some solid combustibles are ignited and then are converted into naked fire after a smoldering phase. At the beginning of the combustion process, the fire volume is very small, and both the burning speed and heat release rate are gradually increased. In the combustion process, fire plumes and ceiling jets [27] are produced, as depicted in Figure 2.

Due to the external forces, the mobility patterns of nodes are given as follows:

(i) *Mobility Pattern of SRNs*. In the smoldering phase, under the external forces of fire plumes, ceiling jets,

gravity and Coriolis force [28], as shown in Figure 3, SRNs will move slowly on the ground because the gravity of nodes is usually large enough. Thus, each SRN is assumed to move at a speed of v_s which falls into the interval (v_{min}, v_{max}), and each SRN resides for a short period of t_s at each time slot, as illustrated in Figure 5(a).

(ii) *Mobility Pattern of LRNs*. In the explosion phase, each node falling in the explosion range r_e of a fire behavior becomes an LRN. Each LRN bounces along the push force direction, and the bounce distance should be smaller than the maximum bounce range r_l (as shown in Figure 4). The bounce of each LRN is repeated after a residence period of t_l, unless it is beyond the explosion range. Specially, if an LRN reaches the boundary of **A**, it bounces off the border with the reflecting direction, as shown in Figure 5(b).

(iii) *Mobility Pattern of FNs*. FNs are assumed to move at a constant speed of v_f. At each time slot, each FN will reside for a period of t_f to detect the nearby fire behaviors. FNs first move to rescue the survivals and then move to extinguish the fire [29]. An example of the FN movements is given in Figure 5(c).

(iv) *Mobility Pattern of RNs*. RNs are deployed to help forward the data packets. Each RN is set to move at a constant speed of R_c/τ. The fire area is divided into some hexagonal cells, as illustrated in Figure 5(d), which indicates that an RN always moves to the adjacent cell with the minimum number of neighbouring untraversed cells. When all of the neighbouring cells are obstacle cells, the RN returns to the last traversed cell to find a neighbouring untraversed cell.

3.2. Position Stability. We give the notion of position stability to measure the position alterations of nodes over time, and the value of position stability can be used to distinguish the types of SRNs and LRNs. The position stability of each node is determined by calculating the position alterations between it and its neighbours; i.e., the position stability of a node becomes smaller when more of its neighbours are changed over time.

The coordinate of V_i at the t-th time slot is expressed as $C(i)^t = (x_i^t, y_i^t)$, and the set of neighbours is denoted by $\mathcal{N}_i^t$. Hence, the Euclidean distance between V_i and a neighbour V_j ($V_j \in \mathcal{N}_i^t$) at the t-th time slot is calculated as $d(i,j)^t = \sqrt{(x_i^t - x_j^t)^2 + (y_i^t - y_j^t)^2}$. The position alteration between V_i and V_j at the t-th time slot is defined as

$$d_p(i,j)^t = \begin{cases} \zeta, & \text{if } V_j \in \mathcal{N}_i^{t-1} \text{ and } V_j \notin \mathcal{N}_i^t, \\ \sqrt{\left[\left(x_i^t - x_j^t\right) - \left(x_i^{t-1} - x_j^{t-1}\right)\right]^2 + \left[\left(y_i^t - y_j^t\right) - \left(y_i^{t-1} - y_j^{t-1}\right)\right]^2}, & \text{otherwise,} \end{cases} \tag{1}$$

where ζ is a large constant. Formula (1) indicates that when V_i and V_j are neighbours during two consecutive time slots (at the $(t-1)$-th time slot and the t-th time slot) the position alteration is calculated as the distance variation between them.

The position stability of V_i at the t-th time slot is denoted by $S_p(i)^t$

$$S_p(i)^t = 1 - \frac{2}{\pi} \cdot \arctan\left\{ \sum_{V_j \in \mathcal{N}_i^{t-1}} \frac{\left[d_p(i,j)^t - \widetilde{d}_p(i)^t\right]^2}{\left|\mathcal{N}_i^{t-1}\right|} \right\}, \tag{2}$$

where $|\mathcal{N}_i^{t-1}|$ denotes the number of neighbours of V_i at the $(t-1)$-th time slot, and $\widetilde{d}_p(i)^t$ denotes the minimum position alteration between V_i and its neighbours at the t-th time slot. Note that the value of $\arctan\{\sum_{V_j \in \mathcal{N}_i^{t-1}}([d_p(i,j)^t - \widetilde{d}_p(i)^t]^2/|\mathcal{N}_i^{t-1}|)\}$ falls into the interval $[0, \pi/2)$, and hence $S_p(i)^t \in (0,1]$. Formula (2) implies that a larger position stability of V_i will be obtained if the position alterations between V_i and its neighbours are smaller.

Besides, we have that

$$\widetilde{d}_p(i)^t = \min_{V_j \in \mathcal{N}_i^t} d_p(i,j)^t. \tag{3}$$

3.3. Proportions of SRNs, LRNs, and FNs in Data Holders. Due to the expensive cost, the number of RNs is extremely small compared with other types of nodes, and we will analyze the optimal proportions of SRNs, LRNs and FNs in data holders in this section.

At each time slot, each data holder forwards the held data packets to κ neighbours, and thus the number of data holders at the t-th time slot is $(\kappa+1)^{t-1}$. To obtain the optimal proportions, the delivery ratio is discussed in four cases: we first analyze the delivery ratio when the data holders are SRNs, LRNs or FNs, respectively, and then the delivery ratio when the data holders are composed of three types of nodes is obtained through combining the conclusions of the aforementioned cases. Note that other cases can also be obtained similarly. The four cases are given as

Case I. $\rho_s = 1$, $\rho_f = 0$ and $\rho_l = 0$, i. e., all data holders are the SRNs. The delivery ratio at the t-th time slot is expressed as

$$\mathscr{D}_s^t = Pr_s + \sum_{k=2}^{t} \left\{ (\kappa+1)^{k-1} \cdot Pr_s \cdot \prod_{i=1}^{k-1} \left[1 - (\kappa+1)^{i-1} \cdot Pr_s\right] \right\}, \tag{4}$$

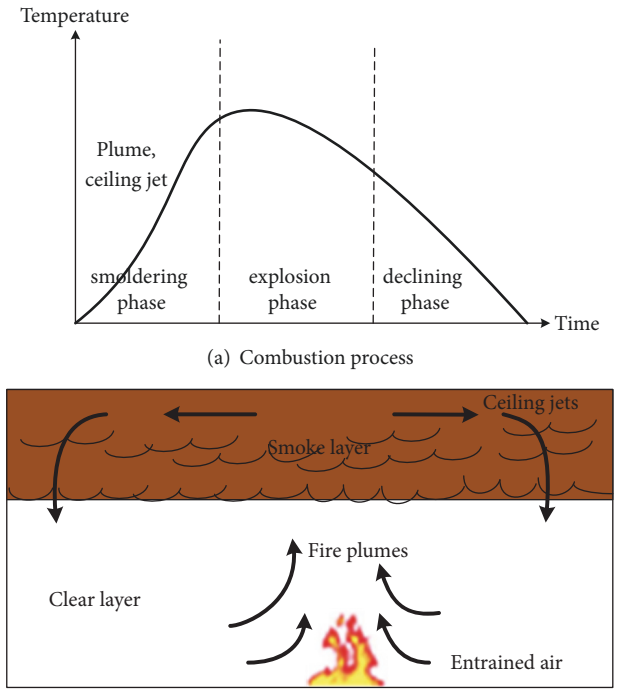

FIGURE 2: Fire plumes and ceiling jets.

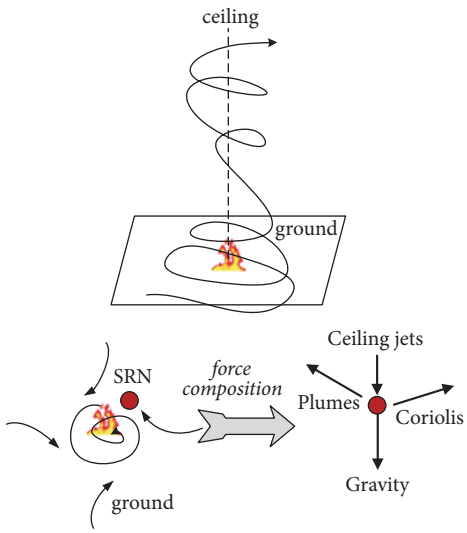

FIGURE 3: External forces in smoldering phase.

where Pr_s denotes the probability of an SRN encountering the RCC. In (4), $(\kappa + 1)^{k-1}$ is the number of data holders at the k-th time slot. Thus, $(\kappa + 1)^{k-1} \cdot Pr_s$ denotes the probability of the data packet being delivered through SRNs at the k-th time slot, and $\prod_{i=1}^{k-1}[1-(\kappa+1)^{i-1} \cdot Pr_s]$ denotes the probability of the data packet not being delivered through SRNs during the previous $(k-1)$ time slots. As illustrated in Figure 6(a), each SRN moves at the speed of v_s and resides for a period of t_s at each time slot, and thus $Pr_s = (2R_c \cdot (\tau - t_s) \cdot v_s)/|\mathbf{A}|$.

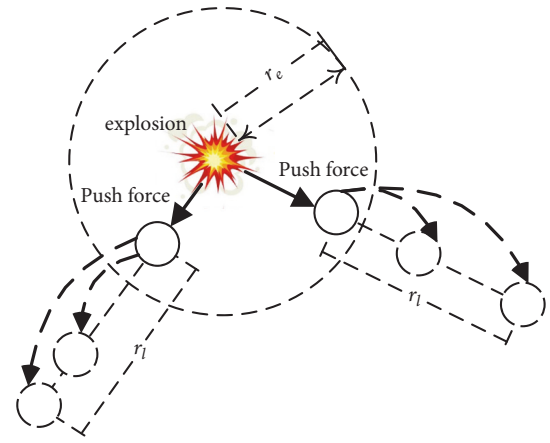

FIGURE 4: Push forces in explosion phase.

Case II. $\rho_l = 1$, $\rho_f = 0$ and $\rho_s = 0$, i. e., all data holders are the LRNs. Likewise, there is

$$\mathscr{D}_l{}^t = Pr_l + \sum_{k=2}^{t} \left\{ (\kappa+1)^{k-1} \cdot Pr_l \cdot \prod_{i=1}^{k-1} \left[1 - (\kappa+1)^{i-1} \cdot Pr_l\right] \right\}, \tag{5}$$

where Pr_l denotes the probability of an LRN encountering the RCC, and $Pr_l = \tau/t_l \cdot (\pi \cdot R_c{}^2)/|\mathbf{A}|$, as shown in Figure 6(b). In (5), $(\kappa + 1)^{k-1} \cdot Pr_l$ denotes the probability of the data packet being delivered through LRNs at the k-th time slot, and $\prod_{i=1}^{k-1}[1-(\kappa+1)^{i-1} \cdot Pr_l]$ denotes the probability of the data packet not being delivered through LRNs during the previous $(k-1)$ time slots.

Case III. $\rho_f = 1$, $\rho_s = 0$ and $\rho_l = 0$, i. e., all data holders are the FNs which move at a constant speed of v_f. We have

$$\mathscr{D}_f{}^t = Pr_f + \sum_{k=2}^{t} \left\{ (\kappa+1)^{k-1} \cdot Pr_f \cdot \prod_{i=1}^{k-1} \left[1 - (\kappa+1)^{i-1} \cdot Pr_f\right] \right\}, \tag{6}$$

where Pr_f denotes the probability of an FN encountering the RCC, and $Pr_f = (2R_c \cdot (\tau - t_f) \cdot v_f)/|\mathbf{A}|$, as illustrated in Figure 6(c).

Case IV. $\rho_s > 0$, $\rho_l > 0$, $\rho_f > 0$ and $\rho_s + \rho_l + \rho_f = 1$. The three types of nodes exist in the data holders simultaneously, and the delivery ratio $\mathscr{D}^t$ can be expressed as

$$\begin{aligned}\mathscr{D}^t = \rho_s \cdot \mathscr{D}_s{}^t \bigcup \rho_l \cdot \mathscr{D}_l{}^t \bigcup \rho_f \cdot \mathscr{D}_f{}^t = \big(&\rho_s \cdot \mathscr{D}_s{}^t + \rho_l \cdot \mathscr{D}_l{}^t + \rho_f \cdot \mathscr{D}_f{}^t - \rho_s \cdot \rho_l \cdot \mathscr{D}_s{}^t \cdot \mathscr{D}_l{}^t - \rho_s \cdot \rho_f \cdot \mathscr{D}_s{}^t \cdot \mathscr{D}_f{}^t - \rho_l \cdot \rho_f \cdot \mathscr{D}_l{}^t \cdot \mathscr{D}_f{}^t + \rho_s \cdot \rho_l \cdot \rho_f \cdot \mathscr{D}_s{}^t \cdot \mathscr{D}_l{}^t \cdot \mathscr{D}_f{}^t\big),\end{aligned} \tag{7}$$

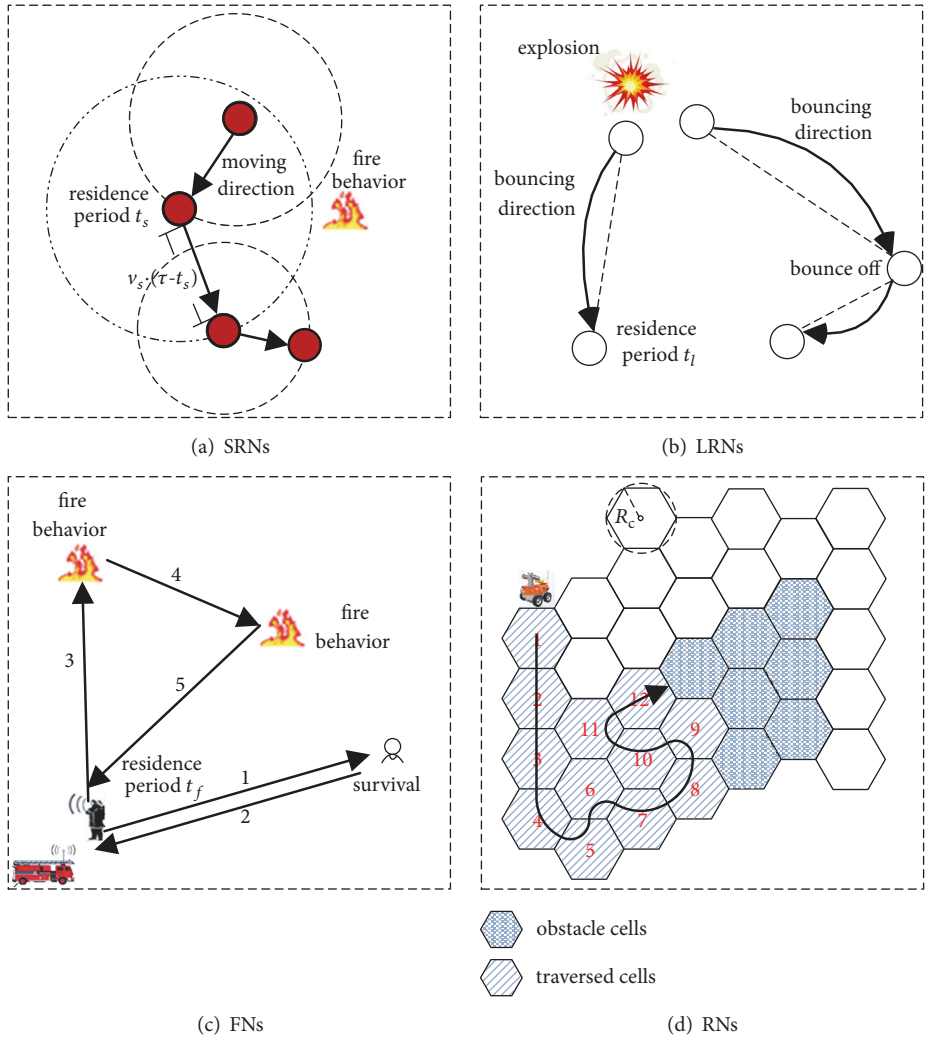

Figure 5: Mobility patterns of SRNs, LRNs, FNs, and RNs.

where $\rho_s \cdot \mathscr{D}_s{}^t$, $\rho_l \cdot \mathscr{D}_l{}^t$ and $\rho_f \cdot \mathscr{D}_f{}^t$ denote the probabilities of the data packet being delivered at the t-th time slot through SRNs, LRNs and FNs, respectively.

The forwarding deadline is $\lfloor \mathscr{T}/\tau \rfloor$, and the expression of delivery ratio before the forwarding deadline is derived by (4), (5), (6) and (7):

$$\begin{aligned}\mathscr{D}^{\lfloor \mathscr{T}/\tau \rfloor} \approx & \sum_{i=1}^{\lfloor \mathscr{T}/\tau \rfloor} (\kappa+1)^{i-1} \\ & \cdot \left(\rho_s \cdot Pr_s + \rho_l \cdot Pr_l + \rho_f \cdot Pr_f\right) \\ & - \left[\sum_{i=1}^{\lfloor \mathscr{T}/\tau \rfloor} (\kappa+1)^{i-1}\right]^2 \cdot \left(\rho_s \cdot \rho_l \cdot Pr_s \cdot Pr_l + \rho_s \cdot \rho_f\right. \\ & \left. \cdot Pr_s \cdot Pr_f + \rho_l \cdot \rho_f \cdot Pr_l \cdot Pr_f\right) \\ & + \left[\sum_{i=1}^{\lfloor \mathscr{T}/\tau \rfloor} (\kappa+1)^{i-1}\right]^3 \cdot \rho_s \cdot \rho_l \cdot \rho_f \cdot Pr_s \cdot Pr_l \cdot Pr_f.\end{aligned} \tag{8}$$

The optimal solutions of ρ_s, ρ_l and ρ_f are denoted by $\overline{\rho}_s$, $\overline{\rho}_l$ and $\overline{\rho}_f$, respectively. $\overline{\rho}_s$, $\overline{\rho}_l$ and $\overline{\rho}_f$ can be obtained by maximizing $\mathscr{D}^{\lfloor \mathscr{T}/\tau \rfloor}$, and the obtained solutions will be used in DFAFR to maintain the optimal proportions of SRNs, LRNs and FNs in data holders approximatively.

3.4. Expected Delivery Delay. With regard to SRNs, the probability of data packets being delivered at the t-th time slot is expressed as $(\kappa+1)^{t-1} \cdot Pr_s$, and thus the expected delivery delay is expressed as

$$\begin{aligned}\tau \cdot \sum_{k=1}^{\lfloor \mathscr{T}/\tau \rfloor} & \left\{k \cdot (\kappa+1)^{k-1} \cdot Pr_s \right. \\ & \left. \cdot \prod_{i=1}^{k-1} \left[1 - (\kappa+1)^{i-1} \cdot Pr_s\right]\right\},\end{aligned} \tag{9}$$

where the part of $\prod_{i=1}^{k-1}[1 - (\kappa+1)^{i-1} \cdot Pr_s]$ denotes the probability of data packets not being delivered during $(t-1)$

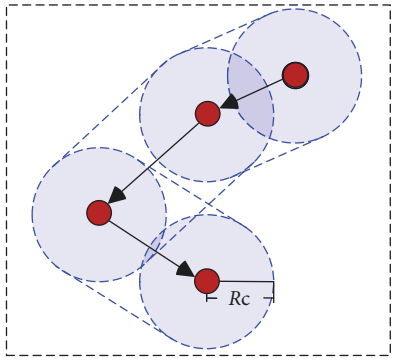

(a) SRNs

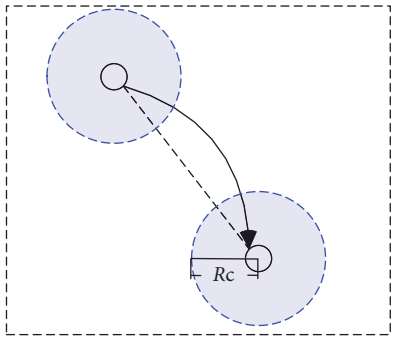

(b) LRNs

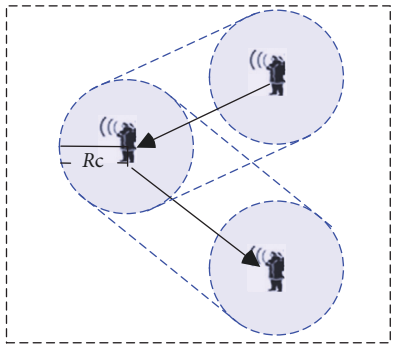

(c) FNs

Figure 6: Communication coverage.

time slots. Likewise, the expected delivery delay of LRNs and FNs is written as

$$\tau \cdot \sum_{k=1}^{\lfloor \mathcal{T}/\tau \rfloor} \left\{ k \cdot (\kappa+1)^{k-1} \cdot Pr_l \cdot \prod_{i=1}^{k-1} \left[1 - (\kappa+1)^{i-1} \cdot Pr_l \right] \right\}, \tag{10}$$

$$\tau \cdot \sum_{k=1}^{\lfloor \mathcal{T}/\tau \rfloor} \left\{ k \cdot (\kappa+1)^{k-1} \cdot Pr_f \cdot \prod_{i=1}^{k-1} \left[1 - (\kappa+1)^{i-1} \cdot Pr_f \right] \right\}. \tag{11}$$

The area of each cell is $(3\sqrt{3}/2){R_c}^2$. For each RN, the expected delivery delay is expressed as

$$\left(\frac{|\mathbf{A}|}{\left(3\sqrt{3}/2\right){R_c}^2} - n_{tr} - n_{ob} \right) \cdot \tau, \tag{12}$$

where n_{tr} and n_{ob} denote the number of traversed cells and the number of obstacle cells, respectively.

The expected delivery delay will be applied to determine the new data holders in DFAFR.

4. Opportunistic Data Forwarding Approach

The typical mobility patterns of nodes are considered in the design of data forwarding approach. In the opportunistic Data Forwarding Approach of Fire-Rescue scenario (DFAFR), each data holder independently forwards the held data packets to the nodes which are selected from the data holder candidates and the adjacent RNs, and the data holder candidates are determined through maintaining the optimal proportions of SRNs, LRNs and FNs in data holders. Note that the optimal proportions are related to the mobility patterns of nodes. Besides, each node probably alters its mobility pattern during the data forwarding process; e.g., an SRN (or an LRN) is probably transformed into an LRN (or SRN) due to the external forces, which is considered in DFAFR as well.

The storage capacities of nodes are usually insufficient, because the capacity of nodal storage modules is extremely limited (the space memory is even measured in KB [30]), and thus some held data packets must be discarded to make room for the arrivals of new data packets. A data packet $data(s,d)$ is assumed to be forwarded from the source node V_s to the destination V_d (RCC), and the detailed description of DFAFR is given as follows:

Step 1. $\overline{\rho}_s$, $\overline{\rho}_l$ and $\overline{\rho}_f$ are obtained from formula (8).

Step 2. At the t-th time slot, each data holder V_i broadcasts an *inquire_msg* containing a quintet $(ID, t, C(i)^t, type, data\_list(i)^t)$, where *type* and $data\_list(i)^t$ denote the node type and the list of held data packets, respectively.

Step 3. After the reception of *inquire_msg* from V_i, each neighbour V_j replies a *reply_msg* which contains the similar information with *inquire_msg*. If V_d has received the *inquire_msg* from V_i, and then V_i sends $data(s,d)$ to V_d immediately.

Step 4. The position stability of each node (excluding the FNs and RNs) is locally computed. Then, each node V_k is classified into an SRN or an LRN according to a stability threshold ξ: if $S_p(k)^t \geq \xi$, and then V_k is an SRN; otherwise, V_k is an LRN. If the new type of V_k is different from that in the quintet of *inquire_msg*, and then a *type_msg* is sent to the neighbours for the type updates.

Step 5. The new data holders will be selected by the following two sub-steps:

(i) Step 5-1. Each data holder V_i selects κ data holder candidates from its neighbours on the basis of $\overline{\rho}_s$, $\overline{\rho}_l$ and $\overline{\rho}_f$ which are obtained from (8) in Step 1.

(ii) Step 5-2. κ new data holders are selected from the data holder candidates and the adjacent RNs according to the expected delivery delay calculated by (9), (10), (11) and (12), i.e., the neighbours with shorter expected delivery delay are selected as the new data holders. Note that all of the κ data holder candidates will become the new data holders if there are no RNs around V_i.

After that, V_i sends $data(s,d)$ to the selected new data holders.

Step 6. If a new data holder V_j receives the $data(s,d)$ from V_i, and then V_j updates the list of held data packets as

$$data\_list\,(j)^{t+1} \longleftarrow data\_list\,(j)^{t} \bigcup data\,(s,d)\,. \quad (13)$$

Specially, if the storage capacity of V_j has been full, the earliest held data packet is discarded to make room for the arrival of $data(s,d)$.

Step 7. Steps 2–6 are repeated until V_d receives $data(s,d)$ or the deadline has been expired. If $data(s,d)$ has been delivered to V_d before the deadline, and then an announcement message originated from V_d will be propagated to all the data holders of $data(s,d)$ to stop their further forwardings and discard all $data(s,d)$ copies. The size of announcement message is very small and can be piggybacked with other messages, and thus the effect of broadcast is negligible. A demonstration of DFAFR execution is given in Figure 7.

The exchanged messages of DFAFR are mainly yielded in Steps 2, 3, 4, and 6. In Step 2, each node broadcasts an *inquire_msg*, and therefore the total message amount will reach N in the worst case; in Steps 3 and 4, there are $N^2 \cdot (\pi \cdot {R_c}^2)/|\mathbf{A}|$ *reply_msg*s and *type_msg*s to be transmitted, respectively; Step 5 makes each data holder forward κ copies of $data(s,d)$, and thus there are utmost $\kappa \cdot (\kappa+1)^{\lfloor \mathcal{T}/\tau \rfloor - 1}$ copies of $data(s,d)$; As a result, the message complexity of DFAFR is at most $\mathbf{O}(N^2)$. Table 2 shows the message complexity of each step in DFAFR.

5. Simulation Evaluation

In this section, DFAFR is evaluated by observing the performance variations with respect to different parameters and by comparing with other algorithms (DT, EF, PROPHET and MPRP). DFAFR is realized in ONE (Opportunistic Networks Environment) [31], which is a simulation environment that can generate the node mobility using different movement models and forward the data packets between nodes with various routing algorithms. The delay for each forwarding is computed as $L_s/B + R_c/\varsigma$ [32], where B is the channel capacity (in bits per second), and ς is the propagation speed of electromagnetic wave.

Table 2: Message complexity of each step.

Step	Complexity
1	O(1)
2	O(N)
3	O(N^2)
4	O(N^2)
5	O(1)
6	O(1))
7	O(1)

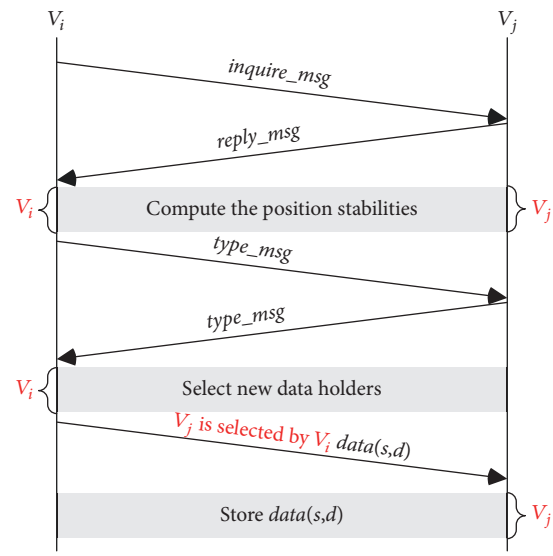

Figure 7: Message exchanges between neighbours.

The deadline is set according to the statistical data provided in an USFA's report "Structure Fire Response Times", which claims that 51% of structure fires confined to room of origin and floor of origin had response times of less than 5 minutes, while 54% of fires confined to building and 49% beyond building had response times of less than 6 minutes. The deadline of data packet delivery should be shorter than the response time, and we set it to 120 seconds (2 minutes). Besides, the capacity of nodal storage modules is extremely limited (the space memory is even measured in KB or MB [30], e.g., the chip CC2430 has a flash memory of 128 KB [33]), and we set $S = 30,000$ KB in the following simulations.

5.1. Environment Settings. The fire-rescue area is with the size of 35m×65m. At the beginning, N nodes (including 15 FNs and 3 RNs) are evenly deployed into the fire-rescue area. Every time slot, 3 explosion locations are randomly selected from all of the fire locations, and the nodes falling into the explosion ranges become LRNs. Each node generates a new data packet with a probability p_g to report the nearby fire behaviors, and these data packets should be forwarded to RCC. The storage capacity of SRNs, LRNs, FNs and RNs is set to 5MB, 5MB, 50MB and 50MB, respectively. The values of other parameters are given in Table 3.

Table 3: Simulation Parameters.

Parameter	Description	Value
N	Number of nodes	100
$\mathcal{T}$	Deadline	120 s
p_g	Probability of a node generating a data packet at each time slot	0.5
R_c	Communication range of each node	8 m
τ	Length of each time slot	20 s
L_s	Size of each data packet	500 KB
S	Storage of each node	30,000 KB
κ	Number of forwarded copies at each time slot	2
(v_{min}, v_{max})	Speed interval of SRNs	(0.1,1.5) m/s
t_s	Residence period of SRNs at each time slot	3 s
t_l	Residence period of LRNs after each bounce	10 s
t_f	Residence period of FNs at each time slot	5 s
v_f	Movement speed of FNs	2.0 m/s
r_e	Explosion range	9 m
r_l	Maximum bounce range	12 m
ξ	Stability threshold	0.4
ζ	Constant in formula (1)	65
ς	Propagation speed of electromagnetic wave	300,000 km/s
B	Channel capacity	8 kbps

5.2. Impacts of Time Slot Length and Data Packet Size. The results regarding the impacts of τ on the total number of data packet copies and the delivery ratio are given in Figure 8. Each node generates a new data packet with the probability p_g at the interval of τ, and thus a smaller τ leads to a larger number of data packets, which makes the network be saturated more easily and depresses the delivery ratio more severely.

Figure 9 illustrates the impacts of data packet size on the delivery ratio, forwarding overhead (Forwarding overhead is defined as the average number of forwarded copies for each delivered data packet, and the index of forwarding overhead can measure the expense of the data packet deliveries.) and delivery delay. Figure 9(a) shows that a larger delivery ratio can be achieved with a smaller data packet size, which is attributed to the fact that more data packets can be propagated and held by nodes when the data packets are with smaller size. Besides, the curve of delivery ratio rises with the increase of N, regardless of the data packet size. This is because more receivers are available when the nodes are deployed more densely, and thus better data holders can be selected to enhance the delivery ratio. In Figure 9(b), the bars of forwarding overhead fluctuate very slightly with the increase of N, which indicates that DFAFR has a good scalability with respect to the forwarding overhead. In Figure 9(c), the curve with a smaller data packet size is much lower than others, and the delivery delay gradually decreases with the increase of N. The reason is that better intermittent paths can be found to shorten the delivery delay when the nodes are deployed more densely.

5.3. Proportions of SRNs, LRNs and FNs in Data Holders. As described in Section 4, DFAFR strives for maintaining the optimal proportions of SRNs, LRNs and FNs in data holders to enhance the delivery ratio. To verify the effect of this mechanism, some simulation results are given in Figure 10. Figure 10(a) shows the optimal solutions $\overline{\rho}_s$, $\overline{\rho}_l$ and $\overline{\rho}_f$ which are calculated by formula (8). Then, we can observe that DFAFR outperforms the results of other proportions (such as $8:1:1$, $7:2:1$ and $6:3:1$, which are given in the form of $\rho_s : \rho_l : \rho_f$) in terms of the number of data packet copies, as shown in Figure 10(b). This is because the optimal proportions can increase the delivery ratio effectively, and thus the number of data packet copies is reduced simultaneously. Moreover, the total number of data packet copies increases with the increase of N, since more nodes generate more data packets. Accordingly, Figure 10(c) shows that DFAFR achieves the largest delivery ratio through adopting the optimal proportions, and this phenomenon tallies with the aforementioned analysis in Section 3.

5.4. Comparisons with Other Algorithms. This simulation compares the delivery ratio, forwarding overhead, delivery delay and network throughput (Network throughput is defined as the total number of data messages

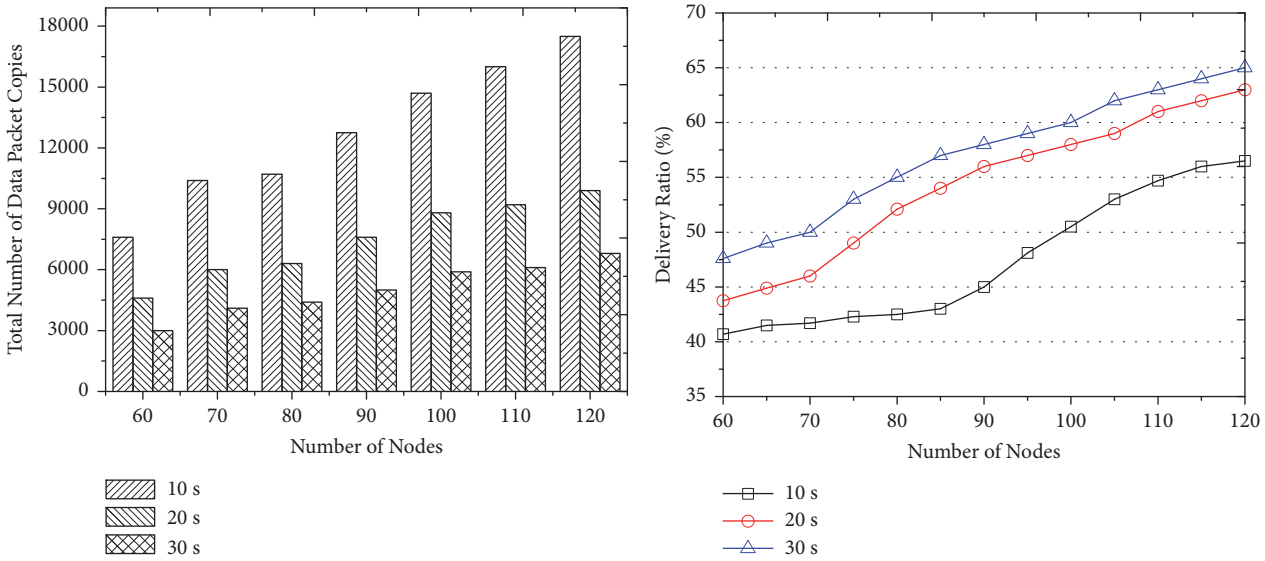

(a) Total Number of Data Packet Copies (b) Delivery Ratio

FIGURE 8: Impacts of time slot length τ.

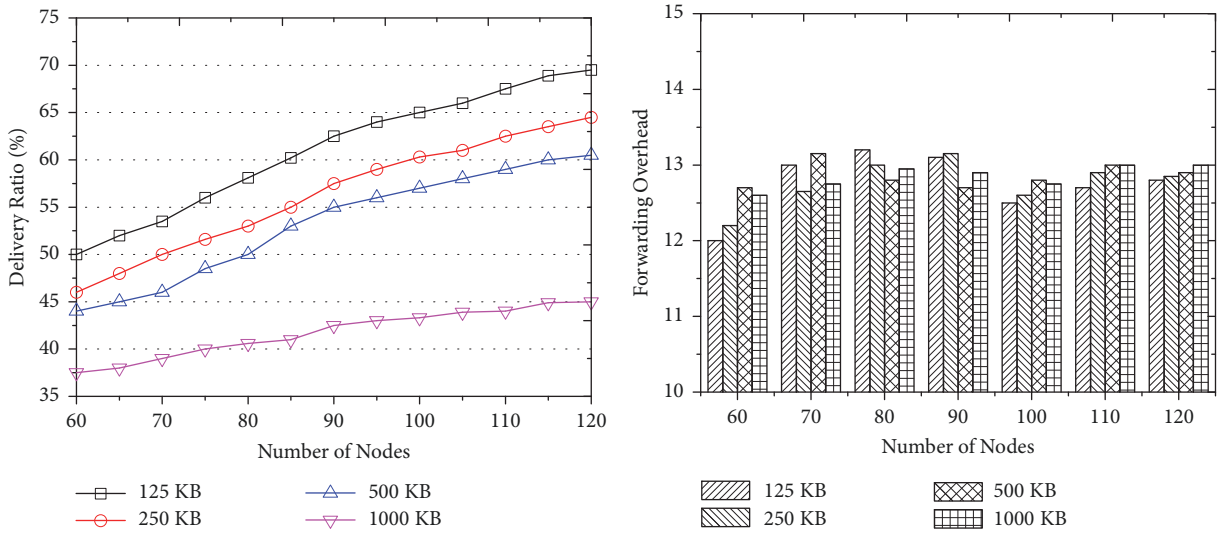

(a) Delivery Ratio (b) Forwarding Overhead

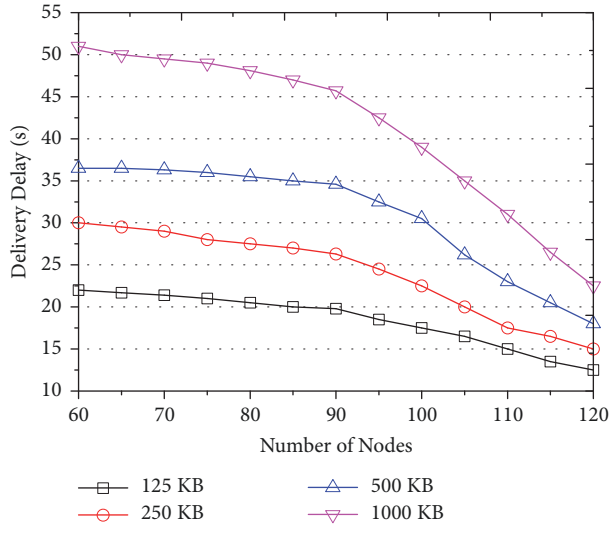

(c) Delivery Delay

FIGURE 9: Impacts of data packet size.

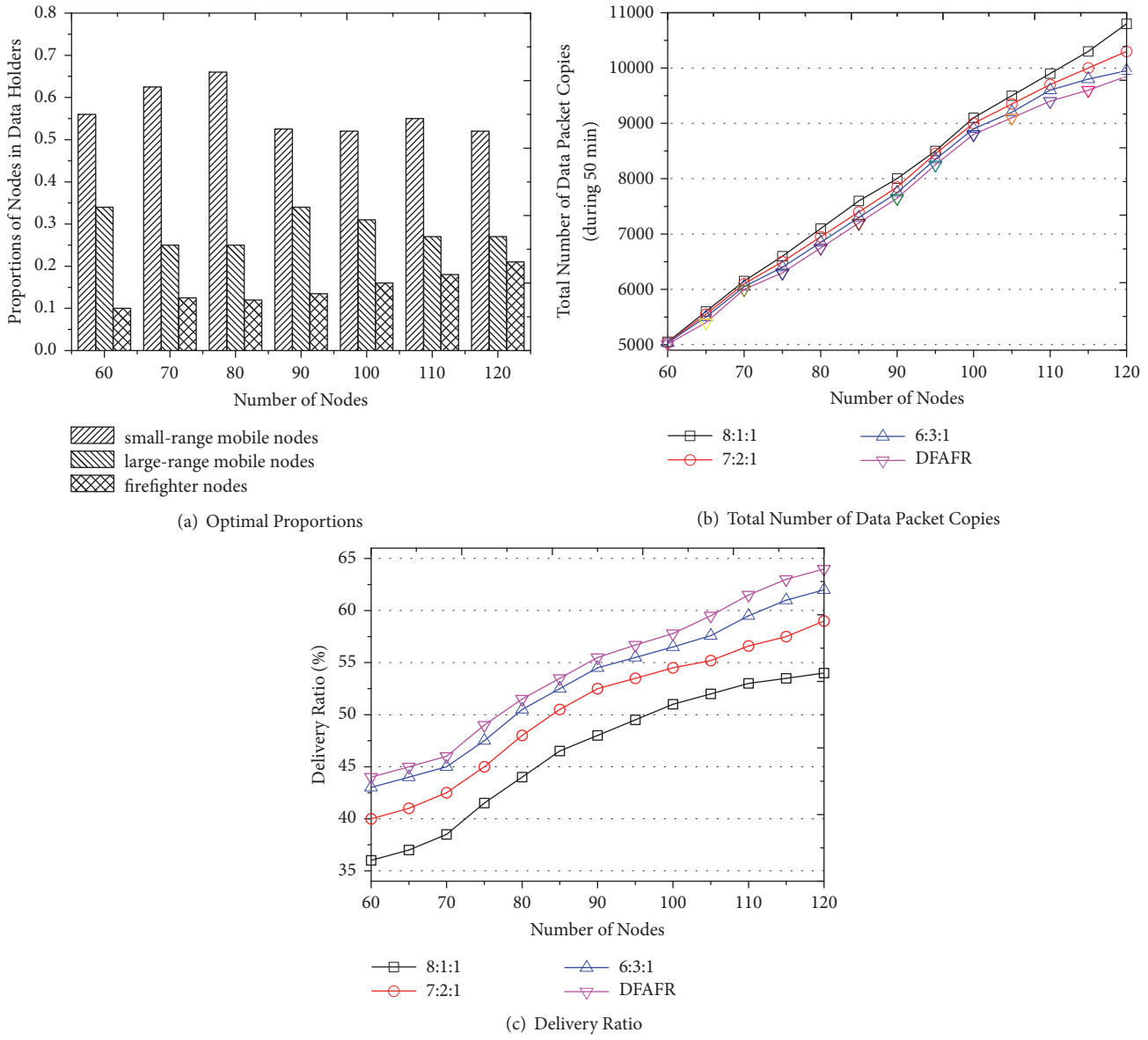

(a) Optimal Proportions

(b) Total Number of Data Packet Copies

(c) Delivery Ratio

FIGURE 10: Impacts of the proportions of SRNs, LRNs and FNs in data holders.

received per unit time by the destinations of all the multi-hop flows in the network) among DFAFR, DT, EF, PROPHET and MPRP, and the results are given in Figure 11.

Some observations are provided as follows: (a) DT achieves the smallest delivery ratio and the largest delivery delay because the source holds the data packets until it encounters the destination node, although the forwarding overhead of DT is much lower than other algorithms. (b) The forwarding overhead of EF is significantly larger than those of other algorithms due to its flooding mechanism. (c) The delivery ratio, delivery delay and network throughput of DFAFR are better than those of other algorithms. The reason is that DFAFR selects the appropriate data holders to enhance the delivery ratio and shorten the delivery delay, and some held data packets are allowed to be discarded by nodes to make room for new data packets. Especially note that the flooding mechanism in EF will make the storage of nodes be rapidly occupied, and many held data packets have to be casually discarded by nodes, thereby decreasing the delivery ratio and prolonging the delivery delay. (d) The forwarding overhead of DFAFR is lower than those of EF, PROPHET and MPRP, and the gaps become large with the increase of N, as illustrated in Figure 11(b).

The above results indicate that DFAFR outperforms other algorithms in terms of delivery ratio, delivery delay and network throughput with a low forwarding overhead. In summary, we give Table 4 to show the differences of DFAFR, DT, EF, PROPHET and MPRP visually.

6. Conclusions

This paper investigates the opportunistic data forwarding problem for OMSNs in the fire-rescue scenario. In

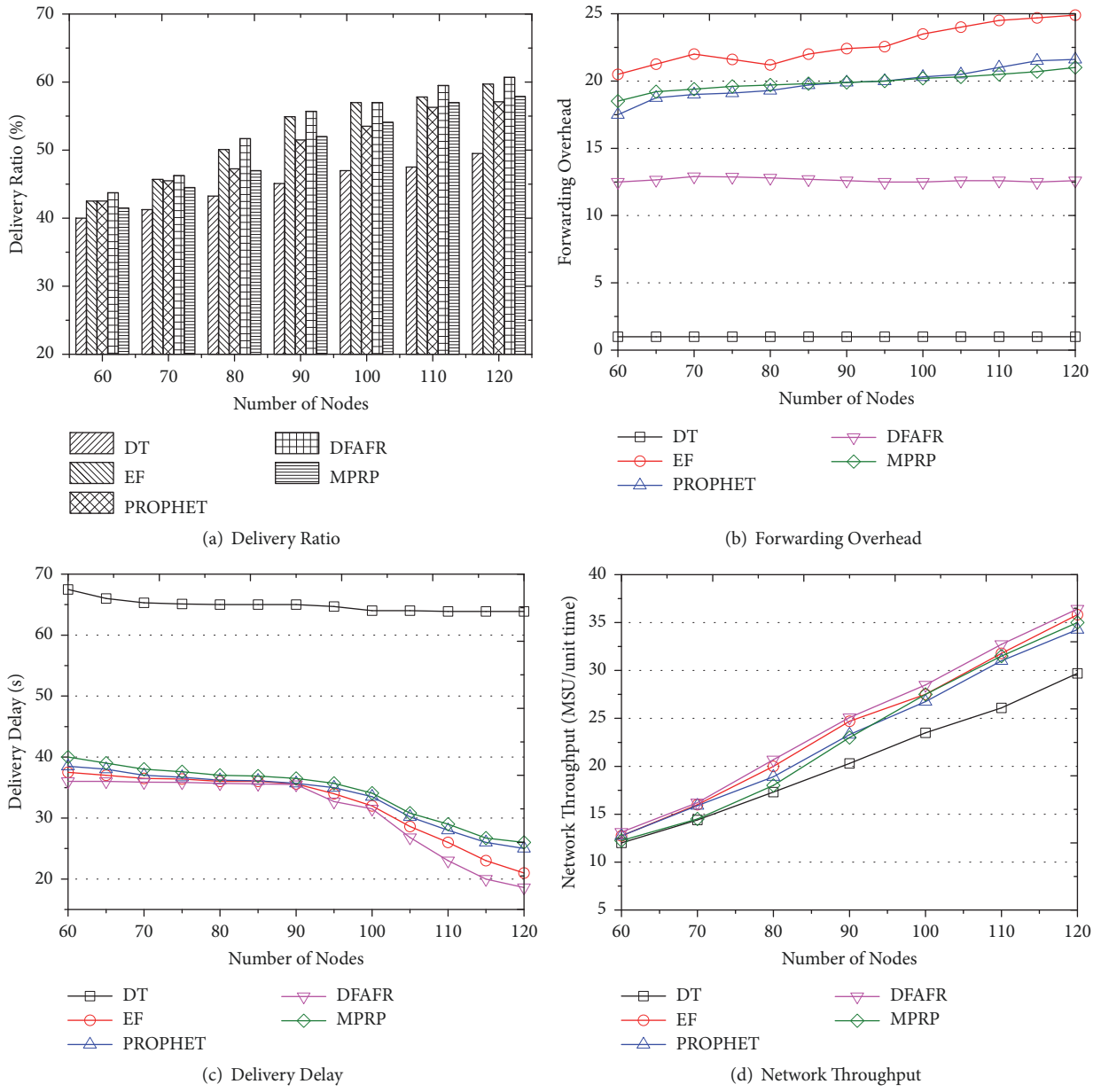

Figure 11: Algorithm comparisons.

Table 4: Comparisons of DFAFR, DT, EF, PROPHET and MPRP.

Algorithm	Forwarding manner	Mobility patterns	Delivery ratio	Delivery delay	Forwarding overhead	Scenario
DFAFR	opportunistic forwarding	multiple types	large	short	low	fire-rescue scenario
DT	direct transmission	single type	small	extremely long	low	delay-insensitive scenario
EF	flooding broadcast	single type	large	short	extremely high	cost-insensitive scenario
PROPHET	probabilistic routing	single type	large	short	low	regular-movent scenario
MPRP	opportunistic forwarding	single type	large	short	low	earthquake-scenario

DFAFR, the types of SRNs and LRNs can be differentiated according to the position stabilities of nodes. DFAFR can enhance the delivery ratio and shorten the delivery delay with a low forwarding overhead, through maintaining the optimal proportions of SRNs, LRNs and FNs in data holders approximatively, and the new data holders are selected from the data holder candidates and the adjacent RNs according to the expected delivery delay.

DFAFR is suitable for the event-emergent scenarios, especially the fire-rescue scenario. Note that in some practical applications the battery capacity of nodes is limited, and some nodes may exhaust their battery energy; besides, some nodes are probably damaged due to the nearby fire behaviors such as explosions. The exhausted nodes or damaged nodes are considered to quit the network, and in these cases the optimal proportions of SRNs, LRNs and FNs in data holders must be recalculated.

Data Availability

The simulation data used to support the findings of this study were supplied by Linfeng Liu under license and so cannot be made freely available. Requests for access to these data should be made to Linfeng Liu, liulinfeng@gmail.com.

Conflicts of Interest

The authors declare that they have no conflicts of interest.

Acknowledgments

This research is supported by National Natural Science Foundation of China under Grant Nos. 61872191, 41571389, 61801215, 61872193.

References

[1] M. di Francesco and S. K. Das, "Data collection in wireless sensor networks with mobile elements: a survey," *ACM Transactions on Sensor Networks*, vol. 8, no. 1, article 7, 2011.

[2] L. He, L. Kong, Y. Gu, J. Pan, and T. Zhu, "Evaluating the on-demand mobile charging in wireless sensor networks," *IEEE Transactions on Mobile Computing*, vol. 14, no. 9, pp. 1861–1875, 2015.

[3] K. Sha, W. Shi, and O. Watkins, "Using wireless sensor networks for fire rescue applications: requirements and challenges," in *Proceedings of the IEEE International Conference on Electro/Information Technology*, pp. 239–244, East Lansing, Mich, USA, May 2006.

[4] J. Luo and Z. Bu, "Design of fire control information transmission system based on internet of things," in *Proceedings of the International Conference on Artificial Intelligence: Techniques and Applications (AITA 2016)*, pp. 19–23, Shanghai, China, 2016.

[5] H. Liu, J. Li, Z. Xie et al., "Automatic and robust breadcrumb system deployment for indoor firefighter applications," in *Proceedings of the 8th Annual International Conference on Mobile Systems, Applications and Services, MobiSys 2010*, pp. 21–34, San Francisco, Calif, USA, June 2010.

[6] A. N. Njoya, C. Thron, J. Barry et al., "Efficient scalable sensor node placement algorithm for fixed target coverage applications of wireless sensor networks," *IET Wireless Sensor Systems*, vol. 7, no. 2, pp. 44–54, 2017.

[7] L. Liu, P. Zhou, J. Wu, R. Wang, X. Fan, and H. Zhu, "A data forwarding approach for opportunistic mobile sensor networks in fire-rescue scenario," in *Proceedings of the 2018 IEEE 22nd International Conference on Computer Supported Cooperative Work in Design (CSCWD)*, pp. 630–635, Nanjing, China, May 2018.

[8] M. Grossglauser and D. N. C. Tse, "Mobility increases the capacity of ad hoc wireless networks," *IEEE/ACM Transactions on Networking*, vol. 10, no. 4, pp. 477–486, 2002.

[9] F. Li and J. Wu, "LocalCom: a community-based epidemic disseminating scheme in disruption-tolerant networks," in *Proceedings of the IEEE Communications Society Conference on Sensor, Mesh and Ad Hoc Communications and Networks (IEEE SECON)*, pp. 574–582, Rome, Italy, June 2009.

[10] A. Lindgren, A. Doria, E. Davies, and S. Grasic, "Probabilistic routing protocol for intermittently connected networks," in *Proceedings of the International Workshop on Service Assurance with Partial and Intermittent Resources*, pp. 239–254, Fortaleza, Brazil, 2004.

[11] T. Camp, J. Boleng, and V. Davies, "A survey of mobility models for ad hoc network research," *Wireless Communications and Mobile Computing*, vol. 2, no. 5, pp. 483–502, 2002.

[12] K. Lee, S. Hong, S. J. Kim, I. Rhee, and S. Chong, "SLAW: self-similar least-action human walk," *IEEE/ACM Transactions on Networking*, vol. 20, no. 2, pp. 515–529, 2012.

[13] Z. Du, P. Hong, and K. Xue, "Hotspot gravitation mobility model," *IEEE Communications Letters*, vol. 16, no. 2, pp. 193–195, 2012.

[14] I. Joe and S. B. Kim, "A message priority routing protocol for delay tolerant networks (DTN) in disaster areas," in *Future Generation Information Technology*, vol. 6485, pp. 727–737, Jeju Island, Korea, 2010.

[15] M. Y. Uddin, H. Ahmadi, T. Abdelzaher, and R. Kravets, "A low-energy, multi-copy inter-contact routing protocol for disaster response networks," in *Proceedings of the 2009 6th Annual IEEE Communications Society Conference on Sensor, Mesh and Ad Hoc Communications and Networks*, pp. 727–737, Rome, Italy, June 2009.

[16] N. Aschenbruck, E. Gerhards-Padilla, and P. Martini, "Modeling mobility in disaster area scenarios," *Performance Evaluation*, vol. 66, no. 12, pp. 773–790, 2009.

[17] G. J. Kost and J. Gerald, "Theory, principles, and practice of optimizing point-of-care small-world networks," *The Journal of Near-Patient Testing & Technology*, vol. 11, no. 2, pp. 96–101, 2012.

[18] B. Jia, S. Liu, T. Zhou, and Z. Xu, "Opportunistic transmission mechanism based on si in mobile crowd sensing networks," in *Proceedings of the 2017 IEEE International Conference on Software Quality, Reliability and Security Companion, QRS-C 2017*, pp. 211–215, Prague, Czech Republic, July 2017.

[19] S. Zhang, X. Wang, Y. Cao, Z. He, and Y. Zhang, "Research on earthquake rescue mobility model and routing strategy based on DTN," *Application Research of Computers*, vol. 31, no. 12, pp. 3833–3836, 2014.

[20] S. Tanwar, S. Tyagi, N. Kumar, and M. S. Obaidat, "LA-MHR: learning automata based multilevel heterogeneous routing for opportunistic shared spectrum access to enhance lifetime of WSN," *IEEE Systems Journal*, pp. 1–11, 2018.

[21] G. S. Aujla, R. Chaudhary, N. Kumar, J. J. Rodrigues, and A. Vinel, "Data offloading in 5G-enabled software-defined vehicular networks: a stackelberg-game-based approach," *IEEE Communications Magazine*, vol. 55, no. 8, pp. 100–108, 2017.

[22] T. Tabirca, K. N. Brown, and C. J. Sreenan, "A dynamic model for fire emergency evacuation based on wireless sensor networks," in *Proceedings of the 2009 Eighth International Symposium on Parallel and Distributed Computing (ISPDC)*, pp. 29–36, Lisbon, Portugal, June 2009.

[23] Z. Wang and Z. Li, "Underground building fire emergency communication network based on mesh networks," in *Proceedings of the 2012 International Conference on Computer Science and Service System (CSSS)*, pp. 914–917, Nanjing, China, August 2012.

[24] A. Qandour, D. Habibi, and I. Ahmad, "Wireless sensor networks for fire emergency and gas detection," in *Proceedings of the 2012 9th IEEE International Conference on Networking, Sensing and Control, ICNSC 2012*, pp. 250–255, Beijing, China, April 2012.

[25] M. Femminella and G. Reali, "An experimental system for continuous users tracking in emergency scenarios," in *Proceedings of the IEEE Global Telecommunications Conference*, Kathmandu, Nepal, 2011.

[26] M. Femminella and G. Reali, "A zero-configuration tracking system for first responders networks," *IEEE Systems Journal*, vol. 11, no. 4, pp. 2917–2928, 2017.

[27] C. Beyler, "Fire plumes and ceiling jets," *Fire Safety Journal*, vol. 11, no. 1-2, pp. 53–75, 1986.

[28] B. E. Potter, "Atmospheric interactions with wildland fire behaviour - II. Plume and vortex dynamics," *International Journal of Wildland Fire*, vol. 21, no. 7, pp. 802–817, 2012.

[29] S. L. Burton, *Performance and Injury Predictability during Firefighter Candidate Training, [Doctoral Dissertation]*, Virginia Tech, 2006.

[30] P. Rawat, K. D. Singh, H. Chaouchi, and J. M. Bonnin, "Wireless sensor networks: a survey on recent developments and potential synergies," *The Journal of Supercomputing*, vol. 68, no. 1, pp. 1–48, 2014.

[31] A. Keranen, J. Ott, and T. Karkkainen, "The ONE simulator for DTN protocol evaluation," in *Proceedings of the 2nd International Conference on Simulation Tools and Techniques (Simutools '09)*, Rome, Italy, article no. 55, March 2009.

[32] N. Kumar, S. Misra, and M. S. Obaidat, "Collaborative learning automata-based routing for rescue operations in dense urban regions using vehicular sensor networks," *IEEE Systems Journal*, vol. 9, no. 3, pp. 1081–1090, 2015.

[33] Z. H. Xin, X. Y. Wu, Q. Zhang, and L. Y. Hu, "Research on the communication of the serial port between the host personal computer and CC2430," *Advanced Materials Research*, vol. 791-793, pp. 1974–1977, 2013.